JTTEE5 18:364–379
DOI: 10.1007/s11666-009-9298-1
1059-9630/$19.00 © ASM International

Bonding Mechanisms in Cold Spraying: The Contributions of Metallurgical and Mechanical Components

T. Hussain, D.G. McCartney, P.H. Shipway, and D. Zhang

(Submitted September 11, 2008; in revised form December 20, 2008)

The mechanism of bonding in cold spraying is still a matter of some debate. In this work, copper has been cold sprayed onto aluminium alloy substrates, the surfaces of which had been prepared in a variety of ways. The coating-substrate bonding was assessed via a novel intermetallic growth method along with adhesive pull-off testing, and related to the substrate preparation method. The bond strength has been rationalized in terms of a modified composite strength model, with two operative bonding mechanisms, namely (i) metallurgical bonding and (ii) mechanical interlocking of substrate material into the coating. In most cases, mechanical interlocking is able to account for a large proportion of the total bond strength, with metallurgical bonding only contributing significantly when the substrate had been polished and annealed prior to spraying. In addition, grit-blasting has been shown to significantly reduce the bond strength compared to other substrate preparation methods.

Keywords adhesion, bond strength, grit-blasting

1. Introduction

Cold gas dynamic spraying (CGDS) is a high rate material deposition process in which powder particles are accelerated in a supersonic jet of compressed gas to high velocities, whereupon they impact with a substrate, deform plastically, and bond to the surface. The supersonic gas jet is produced by use of a converging-diverging de Laval nozzle (Ref 1) and gases such as helium and heated nitrogen are commonly employed. The particles are observed to bond with the substrate when the particle velocity exceeds a critical value (Ref 2-5). Schmidt et al. (Ref 3) reported a critical velocity of ~500 m s^{-1} for a 25 μm copper particle deposited onto a copper substrate. The critical velocity is perceived to be a function of material properties, the particle size, initial impact temperature, and melting temperature (Ref 2, 3). For most of the materials examined to date, the critical velocity is in the range of 150-900 m s^{-1} (Ref 3).

A number of hypotheses have been proposed concerning the mechanism by which bonding takes place in cold spraying. It has been proposed that the first layer of the cold spray coating buildup (i.e., the deposition of particles onto the substrate) involves, first, substrate surface cratering and activation which removes any substrate surface oxide layers and thus allows a particle to bond with the surface (Ref 6, 7). The bonding mechanism is believed to be the result of an adiabatic shear instability at the interface during impact which occurs as a result of high strain rate deformation processes and creates a metal jet consisting of the particle and substrate material (Ref 4, 8-10). It is the formation of this metal jet which, it is proposed, results in the removal of the surface oxide layer and allows true metal to metal contact to be established. Finite element modeling work by Assadi et al. (Ref 2) showed inhomogeneous temperature and strain distributions at the impact interface which suggests that the bonding is confined to only a fraction of the interacting surfaces. Such inhomogeneity could result in incomplete removal of oxide layers between contacting surfaces (Ref 11). Grujicic et al. (Ref 4) modelled the bonding mechanism of a copper particle onto an aluminium substrate, and also an aluminium particle onto a copper substrate. Along with Champagne et al. (Ref 12), they proposed an interfacial material mixing mechanism in cold spraying of copper onto aluminium which results in the formation of interfacial roll-ups and vortices. The interface of the materials is assumed to behave like a viscous fluid. The velocity required for such interfacial instability to be achieved for copper particles impacting a 6061 aluminium alloy was calculated to be 500 m s^{-1}.

Experiments using transmission electron microscopy have also been conducted to examine the oxide layer between individual particles in both copper and aluminium deposits and its effect on bond formation (Ref 13-15). Evidence of ruptured oxide film was found in the coating. Li et al. (Ref 9) also examined the effect on bond formation of the surface oxide layer present on both an aluminium feedstock powder and an aluminium substrate. It was found that with increasing oxide layer thickness, particle deformation was restrained and formation of the metal jet (seen as a necessary precursor to bond formation) became difficult.

T. Hussain, D.G. McCartney, P.H. Shipway, and **D. Zhang**, University of Nottingham, Nottingham, UK. Contact e-mail: philip.shipway@nottingham.ac.uk.

To date, the effect of substrate surface preparation in bond formation has not been investigated widely. Marrocco et al. (Ref 16) explored the effect of different surface preparation techniques in controlling the bond strength of a cold-sprayed titanium coating on Ti6Al4V. They proposed that grit-blasting of the Ti6Al4V substrate caused work hardening, which subsequently limited its deformation during impact of a titanium particle during cold spraying; it was argued that this restriction of substrate deformation resulted in less effective removal of surface oxide and thus led to lower bond strengths being observed. Wu et al. (Ref 17) studied an Al-Si coating, cold sprayed onto both polished and grit-blasted mild steel. Micro-pores and defects were found in the grit-blasted surface while an ''intimate'' interface was found following deposition onto a polished substrate; it was argued that the micro-pores on the grit-blasted surface resulted in lower bond strengths being observed. They also reported higher bond strength with increasing particle incident velocity. In contrast to the work of Marrocco et al. (Ref 16) and Wu et al. (Ref 17), Makinen et al. (Ref 18) found higher bond strengths for a copper deposit cold sprayed onto a grit-blasted copper surface compared to that observed for deposition onto an as-received surface.

The effect of substrate surface preparation on the deposition efficiency of the process has also been assessed. Sakaki et al. (Ref 19) reported a slight increase in the deposition efficiency in cold sprayed copper and titanium by increasing substrate surface roughness (grit-blasted substrate compared to polished substrate). Richer et al. (Ref 20) also reported an increase in deposition efficiency in spraying an aluminium alloy particle onto a coarser grit-blasted surface when compared to a finer grit-blasted surface. However, the substrate surface roughness has an effect only on the first few layers of coating deposited, and as such, the effect on deposition efficiency may be small, depending upon the significance of the coating initiation stage in the total time for coating development.

The process of coating build up after the initiation stage can also be considered in similar terms to that for particle-substrate interactions. To characterize the interparticle bond formation in cold-sprayed deposits, etching of the microstructure has been commonly used. Stoltenhoff et al. (Ref 21) used etching and image analysis to identify the metal to metal contact between copper particles sprayed with both helium and nitrogen. While this etching technique provided useful insight into the mechanisms of bond formation, control of the etching behavior to obtain reproducible results is very difficult. Price et al. (Ref 11) proposed an alternative method to characterize the interparticle bond formation in cold spraying; here, a blended powder of copper and aluminium particles was cold sprayed and subsequently annealed at 400 °C. It is known (Ref 22-24) that the formation of intermetallic phases during annealing of aluminium-copper diffusion couples indicates that the surfaces in contact are free of oxide layers, and Price et al. (Ref 11) thus utilized the formation of such intermetallics between copper and aluminium particles within the coating as an indicator of metal-to-metal bonding where surface oxide films had been removed during spraying. They observed that the degree of metal to metal contact increased as particle impact velocity in the cold spray process increased.

In the current study, the interfacial bonding between an aluminium substrate and a cold-sprayed copper deposit was examined in detail. The methodology proposed by Price et al. (Ref 11), i.e., using a short heat treatment to promote interdiffusion and intermetallic formation, formed an important part of the work. Furthermore, the aluminium substrate was prepared in a variety of ways to allow an understanding of the basic processes by which bonding is promoted at such interfaces to be obtained. An additional aim was to ascertain how bonding can be most efficiently promoted in the cold spray process.

2. Experimental Procedure

2.1 Materials

Commercial purity (>99 wt.%) copper powder (Sandvik Osprey, Neath, UK) with a size range of −25 + 5 μm was used to produce the coating. The copper powder was deposited onto samples cut from a single 6082 aluminium plate (1.00 wt.% Si, 0.7 wt.% Mn, 0.9 wt.% Mg, 0.2 wt.% Fe, Balance Al), sample dimensions being 38 × 15 × 7 mm.

2.2 Substrate Preparation and Characterization

The aluminium substrates were prepared with three different procedures as follows (termed ground, polished, and grit-blasted, respectively):

(a) ground with 58.5 μm SiC paper;
(b) ground with 58.5, 35, 21.8, and 15.3 μm SiC paper. Polished with 6 and 1 μm diamond grit on soft cloth wheels. Polished with 0.1 μm colloidal silica final polishing suspension;
(c) grit-blasted with Al_2O_3 with grit size of ~500 μm.

The surface roughness (Ra) following each of the three preparation routes was measured using a vertical scanning interferometer (Fogale Nanotech Photomap 3D, Ville Active, Nimes, France), with a 1265 × 945 μm measurement area. From this area three equally spaced line scans of 1265 μm in length were extracted and the Ra value measured. These Ra values were then averaged to provide the Ra for the surface. The hardness of the substrate was measured using a Leco M400 microhardness tester (Cheshire, UK) using a 25 gf load.

It was recognized that the surface preparation of the aluminium substrates would not only change the profile of the surfaces, but may also result in different levels of cold work. As such, following surface preparation by each of the three routes described, a number of the samples were annealed at 450 °C for 1 h. The heat treatment was performed in a tube furnace (Lenton Furnaces, Sheffield, UK) with a protective argon atmosphere. The samples

were heated at 20 K/min and after annealing furnace cooled to room temperature.

2.3 Sample Manufacture

Cold gas spraying was performed with an in-house built cold gas spraying system at the University of Nottingham. The martensitic steel de Laval nozzle had a throat diameter of 1.35 mm, with an area expansion ratio of ~8.8. The system utilized room temperature helium at 2.9 MPa for the primary accelerating gas and nitrogen as the powder carrier gas. The pressure of the carrier gas was set approximately one bar higher (~3.0 MPa) than the primary gas pressure to ensure powder transport into the main flow. A high pressure powder feeder (Praxair 1264HP, Indianapolis, IN, USA) was used during the cold spraying process, with a 120 holes feeding wheel rotating at 4 rpm. The nozzle-substrate standoff distance for all the spray runs was fixed at 20 mm.

All substrates were rinsed with methyl alcohol and dried using compressed air immediately prior to spraying. Substrates (one of each of the different surface preparation routes in both the as-prepared and annealed conditions) were then clamped side-by-side on an X-Y traverse table which controlled the relative motion between the nozzle and the sample. The table moved the samples at 100 mm s^{-1} relative to the nozzle. The schematic of the University of Nottingham cold spray system has been described elsewhere (Ref 25). Photographs of the rig and the detailed description of the installation are available in Calla's thesis (Ref 26). Copper was deposited using a series of linear passes over an area of 18 × 45 mm on each sample type; to achieve uniform coverage, the table was indexed 2 mm between adjacent tracks. The deposit was built up using a number of passes to create a deposit thickness of around 400 μm. In order to manufacture samples for bond strength pull-off tests, coating was sprayed onto all the different types of aluminium substrate using a mask with circular cut-outs of 8.16 mm diameter. The dimensions of the substrate for bond strength testing were 20 × 15 × 7 mm.

2.4 Post-Spray Heat Treatment

Following coating deposition onto the substrates, samples were heat treated to allow formation of copper-aluminium intermetallics at the interfacial regions where the oxides had been disrupted during the spraying process. This heat treatment was performed at 400 °C for 15 min in the tube furnace, surrounded by a stream of continuously flowing high-purity argon gas. The samples were heated at 20 K/min to the annealing temperature, held there for 15 min, and then furnace cooled to room temperature.

2.5 Bond Strength Testing

The bond strength of the as-sprayed deposits was measured using a pull-off adhesion test machine from DFD instruments (Woking, Surrey, UK). The specimen holder is designed to apply uniform stress distribution over the area under test. A thermal cure resin, E1100S supplied by DFD instruments (Woking, Surrey, UK), was used, which itself had a tensile strength of around 80 MPa. A steel pull rod (the dolly) was bonded to the top surface of the coating; the dollies were ground using a coarse SiC abrasive paper and cleaned using methyl alcohol prior to application of the adhesive. After applying the adhesive, samples were put in a vacuum desiccator to remove any air bubbles trapped in the adhesive and then cured in a fan-assisted oven at 120 °C for 90 min. Five pull-off tests were performed for each substrate type, with the mean and standard error in the mean of these five measurements being quoted. Following pull-off testing, the fractured surfaces were examined by SEM.

2.6 Sample Characterization

Coating cross-sections were prepared by cutting samples with a diamond slitting wheel; sections were sequentially ground using SiC paper and then polished to 1 μm diamond surface finish. A FEI XL30 (FEI Europe, Eindhoven, The Netherlands) scanning electron microscope (SEM) operated at 20 kV was employed to examine the microstructure of the coatings using backscattered electron (BSE) imaging, where contrast results from differences in the mean atomic number of the materials being imaged.

Energy dispersive x-ray (EDX) analysis was carried out in the SEM to identify the intermetallics generated during annealing at the interface of copper and aluminium. To quantify the extent of the coverage of the intermetallic phase formed during annealing at the coating-substrate interface, image analysis software (ImageJ, U.S. National Institute of Health, MD) was employed. For each condition, eight representative BSE images of the coating-substrate interface microstructure were selected for measurement; each image had a field of view of approximately 300 × 225 μm.

3. Results

3.1 Characterization of Feedstock Powder

Figure 1(a) shows the morphology of the feedstock copper powder. It can be seen that the particles have a rounded morphology with only a small fraction exhibiting satellite particles. The particle size analysis (Fig. 1b) measured by laser diffractometry (Laser Mastersizer, Malvern Instruments, Malvern, UK) indicates that 92% of the particles are in the specified size range of −25 + 5 μm with approximately 6 vol.% below 5 μm and 2 vol.% above 25 μm.

3.2 Characterization of Different Substrate Surfaces

The roughness of polished, ground, and grit-blasted aluminium substrates was 0.05, 0.4, and 3.9 μm, respectively. Observations of the substrate following grit-blasting showed the presence of embedded alumina grit in some cases. Figure 2 shows the typical surface profiles of the

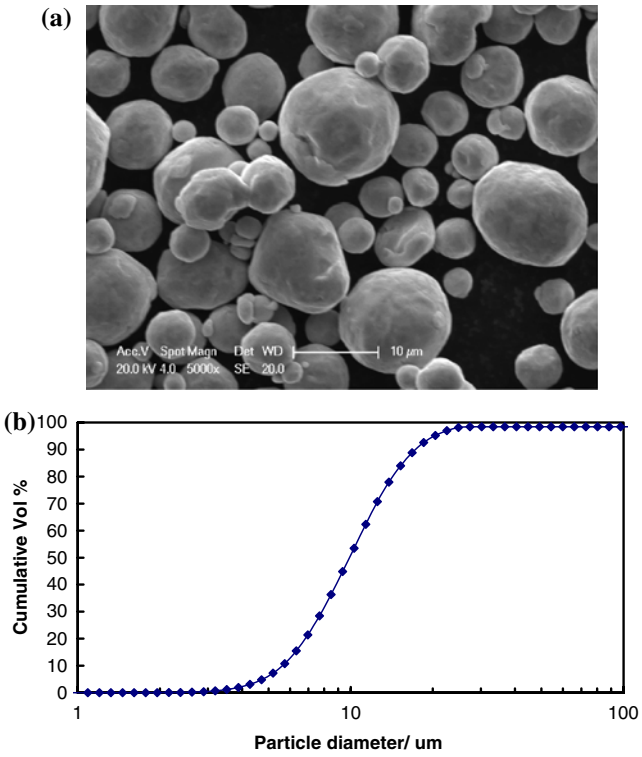

Fig. 1 (a) SE image of gas atomized Cu powder showing its morphology. (b) Cumulative size distribution of copper powder measured by laser diffractometry

substrate following the three surface preparation methods. The typical peak-to-trough height of the grit-blasted surface was ~20 μm, whereas the peak-to-trough height of the polished surface was less than 1 μm. The surface profile of the ground surface shows uniformly distributed peaks and valleys with a typical peak-to-trough height of 3 μm. Figure 3 shows the magnified profiles of the three surfaces in relation to a 15 μm spherical particle.

To identify any surface hardening during the surface preparation of the samples, microhardness indentations were made on a finally polished cross section. Ten hardness measurements were taken within 10 μm of the prepared surface (referred to as near-surface hardness) and ten measurements made at the same load in the centre of the substrate (typically >3 mm from the prepared surface). In a similar manner, the hardnesses of the bulk and surface regions following the annealing heat treatment were measured. The annealing treatment reduced the hardness of the bulk material from 115 to 40 kgf mm^{-2}. The measured near-surface hardnesses are shown in Table 1. It can be seen that in the case of the as-prepared material, the hardnesses of both the ground and polished surface regions were very similar to that of the bulk material. However, grit-blasting resulted in significant hardening of the surface. To compare with these, a sample of 6082 alloy was cold rolled to a strain of ~360%; the hardness of this cold rolled materials was 132 kgf mm^{-2}. It can be seen that this value is significantly lower than that of 179 kgf mm^{-2} measured for the grit-blasted sample. Following annealing, the hardness of the polished and ground surface regions were similar to that of the bulk but the hardness of the annealed, grit-blasted surface was significantly higher than that of the bulk (50 kgf mm^{-2} as opposed to 40 kgf mm^{-2}). Nevertheless, it was greatly reduced compared to that before annealing. A discussion of these results is presented in Sect 4.2.1.

3.3 Bond Strength Tests and Fracture Surface Analysis

3.3.1 Bond Strength Tests. Values for the pull-off bond strength for the copper sprayed onto the aluminium substrate, as a function of the preparation method of the substrate, are presented in Table 2. The values of the bond strength of cold sprayed copper on aluminium reported in Table 2 are in reasonable agreement with the values reported by other researchers (Ref 21, 27, 28). For the as-prepared substrates (i.e., without an annealing treatment following the surface preparation), the bond strength was greatest with the polished surface and lowest with the grit-blasted surface. Similar behavior of reduced bond strength with grit-blasting has been reported for the deposition of titanium by cold spraying (Ref 16).

Table 2 also shows that for polishing or grit-blasting, the bond strength was significantly increased by annealing of the substrate prior to copper deposition. In the pull-off tests for copper deposited onto polished and annealed substrates, the failure was always in the adhesive between the copper and the dolly (rather than between the copper and aluminium); as such, the values recorded simply indicate a lower bound of the bond-strength of the copper-aluminium interface. However, for the ground surface, little change occurred when the substrate was annealed prior to deposition.

3.3.2 Fracture Surfaces. The fracture surfaces following the pull-off tests were examined, and are shown in Fig. 4 for the as-prepared surfaces, and in Fig. 5 for the annealed substrates. In each case, both the aluminium substrate and copper deposit surfaces are shown. In addition, the fractional area of aluminium on the fracture surface of the copper deposit along with the complimentary measure of copper on the aluminium substrate fracture surface are shown in Table 3. Looking at the aluminium substrates, it is clear that copper particles (regions of high brightness) are observed to adhere both as single particles and as groups of particles (Fig. 4a-c and 5a, b); no significant differences were noted in the amount of copper particles retained as a function of the methods of preparation of the aluminium substrate (Table 3). On the surfaces of the copper deposits, aluminium is clearly observed (regions of low brightness). For the polished and ground samples, aluminium is observed primarily in between the copper particles (Fig. 4d, e and 5c). The aluminium has the appearance of being extruded between the copper particles as shown by the higher magnification image of Fig. 6. In contrast to this, the observations for the grit-blasted surfaces show that the aluminium is found more widely dispersed on the copper deposit fracture surface and in larger areas (Fig. 4f and 5d). It is notable

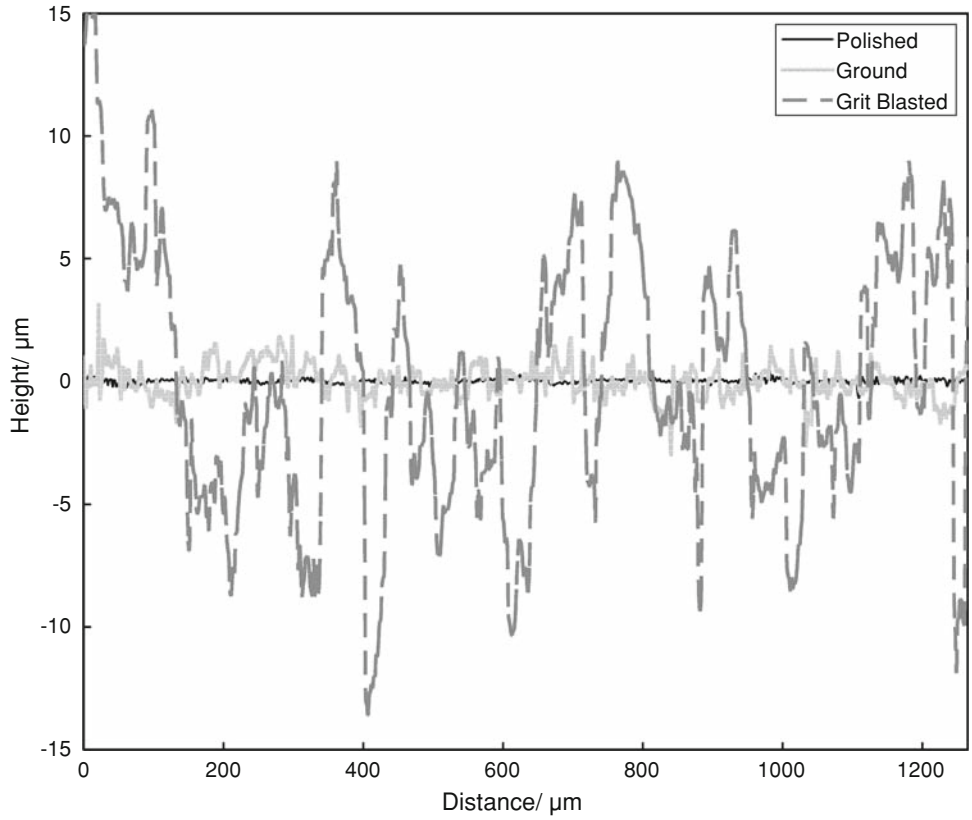

Fig. 2 Typical line profiles extracted from the polished, ground, and grit-blasted surfaces

that for the grit-blasted substrates, the fraction of aluminium visible on the deposit surface is significantly greater than for polished or ground surfaces. Also, it has a different morphology of flat irregular particles as opposed to the solely interparticle presence in polished or ground substrates. This is the case irrespective of whether or not the substrate was annealed before copper deposition.

It is also notable that the fracture surfaces of both the copper deposits and the aluminium substrates show the clear rounded morphology of the copper particles for both the polished and ground surfaces (Fig. 4a, b, d, e and 5a, c), indicating that plastic deformation upon impact was primarily within the aluminium substrate. In contrast, following spraying onto grit-blasted aluminium, the fracture surfaces of both the copper deposits and the aluminium substrates indicate significant deformation (flattening) of the copper particles on impact, irrespective of whether the aluminium substrate was hard (~179 kgf mm^{-2} in the as-grit-blasted state) or soft (~50 kgf mm^{-2} in the annealed state) (Fig. 4c, f and 5b, d).

Table 3 shows the area fractions of aluminium retained on the copper deposit fracture surface and copper retained on the aluminium substrate fracture surface. It is clear that when fracture occurs, the fraction of copper that is retained on the substrate surface is low (around 10%) and generally independent of substrate preparation method or whether or not it had been annealed. The amount of aluminium retained on the surface of the copper deposit depended upon the surface preparation route (although not significantly on whether the substrate had been annealed or not following its preparation). For the polished and ground substrates, around 12% of the area was retained aluminium (primarily retained between copper particles as outlined previously in Fig. 4d, e and 5c). Around 23% of the surface was retained aluminium in the case of deposition onto the grit-blasted surfaces and this aluminium was widely distributed across the fracture surface (Fig. 4f and 5d).

3.4 Microstructural Analysis of Bond Formation

Figure 7 shows cross-sections of the interface regions following deposition of the copper coating onto the as-prepared polished, ground, and grit-blasted aluminium substrates. The copper particles give brighter contrast in the BSE images due to the higher atomic number of copper. In all cases, the coating showed very little porosity with good inter-particle contact. Deformation of the aluminium substrate by cold sprayed copper particles is evident at the interface. In the case of the deposits onto both the polished and ground substrates (Fig. 7a, b), significant deformation of the substrate is observed with the rounded shapes of the copper particles being preserved (in line with the fractographs presented earlier). However, following spraying onto the grit-blasted substrates (Fig. 7c), the general profile of the grit-blasted surface can be observed

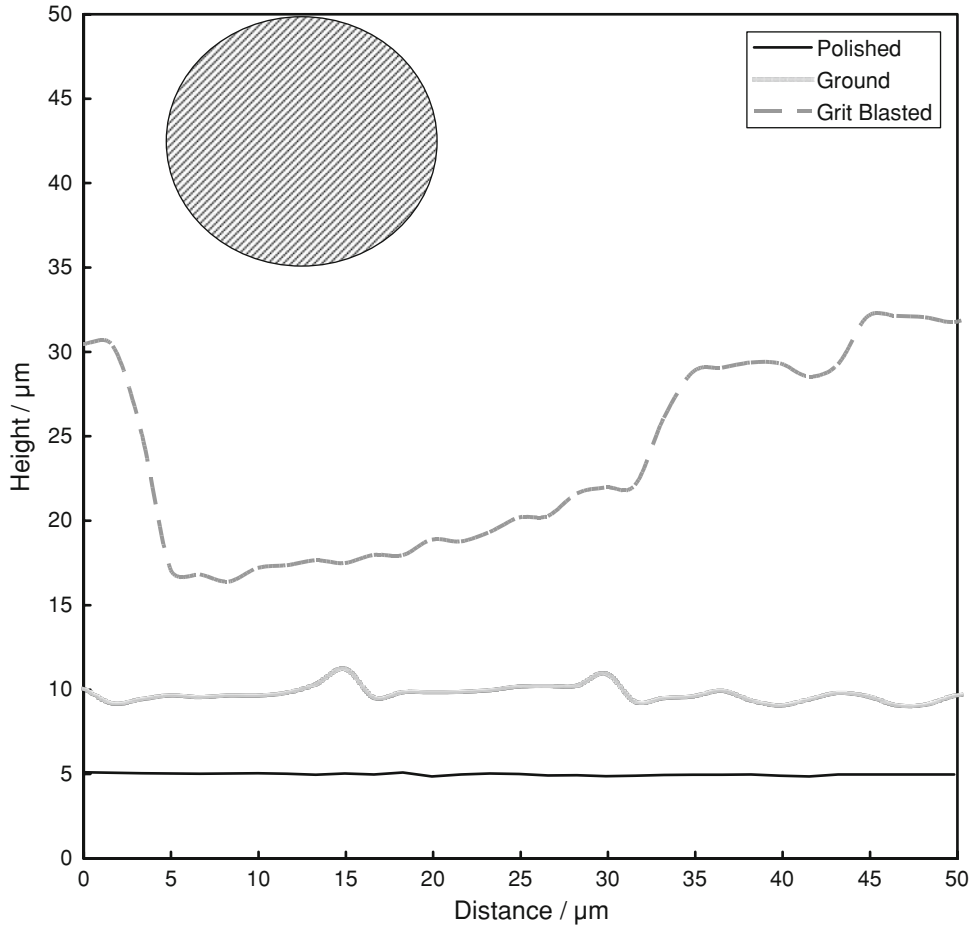

Fig. 3 Surface profiles of polished, ground, and grit-blasted surfaces (with identical horizontal and vertical scaling) in comparison with a disk representing a section through a 15 µm diameter spherical particle

Table 1 Near-surface hardness and surface roughness of the aluminium substrates as-prepared and following annealing

Preparation method	Surface roughness (Ra), µm	Vickers microhardness (25 gf load), kgf mm^{-2}	
		As-prepared	Annealed
Polished surface	0.05	114.5 ± 1.0	38.9 ± 0.3
Ground surface	0.4	105.9 ± 2.4	35.4 ± 0 .5
Grit-blasted surface	3.9	179.1 ± 12.3	50 ± 1.2

The hardness values of the bulk aluminium were 115 ± 1 and 40 ± 1 kgf mm^{-2} in the as-prepared and annealed conditions, respectively

Table 2 Bond strength values for the copper deposited onto aluminium substrates for as-prepared surfaces and following annealing treatment

Substrate surface preparation	Bond strength (as-prepared substrate), MPa	Bond strength (annealed substrate), MPa
Polished surface	57.4 ± 5.3	>69.2
Ground surface	55.9 ± 4.0	59.4 ± 4.5
Grit-blasted surface	35.5 ± 4.7	56.6 ± 2.9

(with undulations on the length scale of ~100 µm, but local deformation of the substrate due to particle impact is not as clear, indicating that the particles themselves underwent significant deformation (in preference to substrate deformation) on impact.

Figure 8 shows cross-sections of the interface regions following deposition of copper coating onto the substrates which had been annealed following surface preparation, as a function of surface preparation method. In all cases, more significant deformation of the aluminium substrate close to the interface is observed, associated with the softening of the substrate due to annealing (see Table 1). However, it is still notable that the shape of the particles close to the interface cannot be clearly observed following deposition onto the grit-blasted and annealed surface, indicating preferential deformation of the particle in this case.

Heat treatment to form Cu-Al intermetallics has been used previously as a means to identify regions where intimate aluminium-copper contact exists (where the intermetallic grows readily) and regions where the metals are separated by oxide films (where intermetallic growth is restricted) (Ref 11). Thus, the coated substrates were heat treated at 400 °C to investigate the degree of intermetallic phase formation.

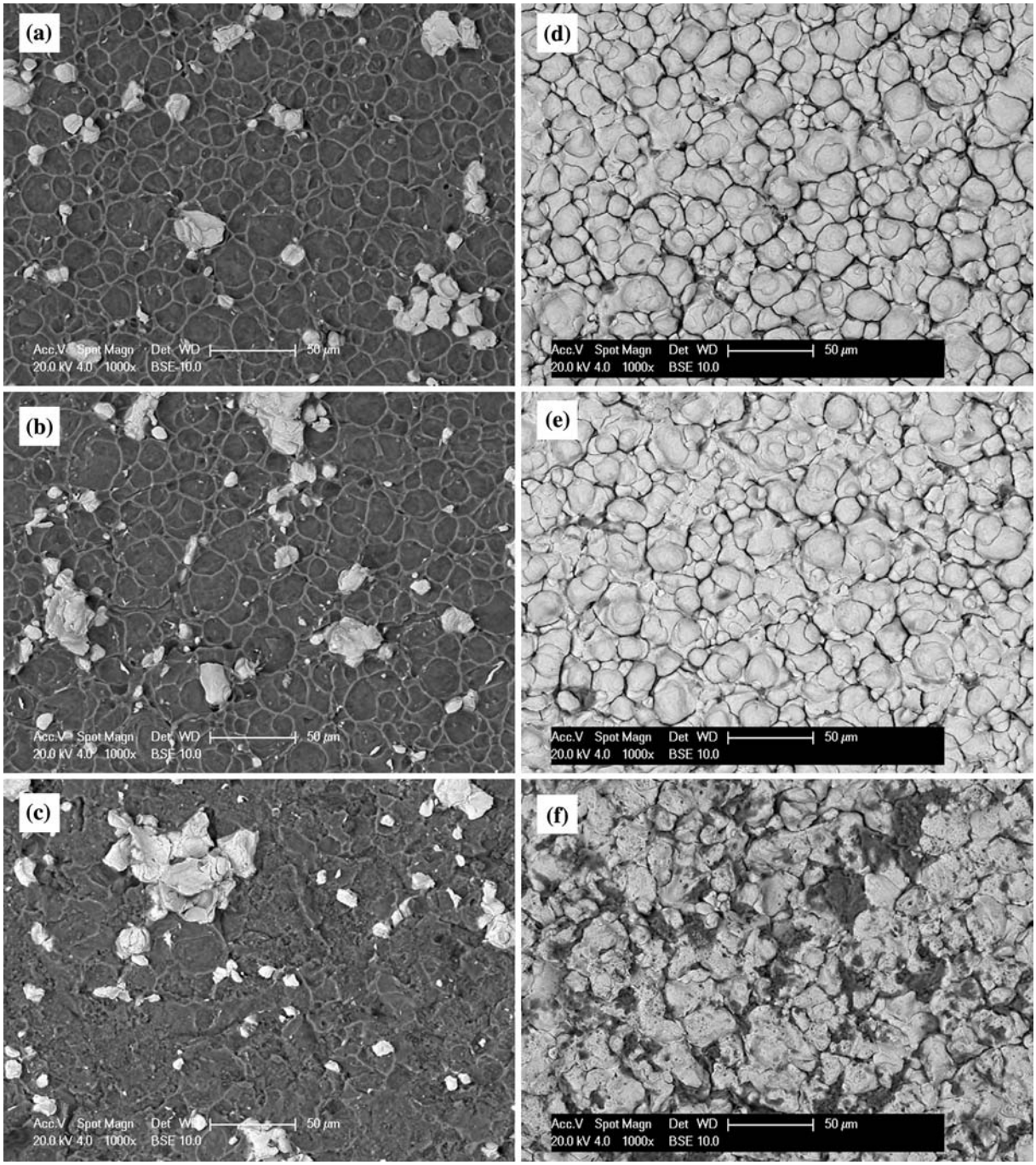

Fig. 4 Fracture surfaces, after pull-off test, of as-prepared Al substrate (a-c) and corresponding copper coating (d-f) with different substrate surface preparations: (a, d) polished; (b, e) ground; and (c, f) grit-blasted. The bright phase is Cu and the darker one Al. The Al substrates show the presence of individual Cu particles adhered to them and the Cu coatings show Al trapped in between Cu particles

Figure 9 shows cross-sections of the interface regions following heat treatment for copper deposited onto the as-prepared polished, ground, and grit-blasted aluminium substrates. Cu-Al intermetallics are identified as the regions with mid-grey contrast between the substrate and the deposit. The intermetallics at the interface grew to a few microns thick in some places, but the coverage of the interface by intermetallics is seen to be limited. Figure 10 shows cross-sections of the interface regions (following heat treatment) for copper deposited onto the aluminium substrates which had been annealed after surface preparation. The intermetallic coverage of the interface is evidently more extensive compared to the equivalent surface preparation (but without an annealing step before copper

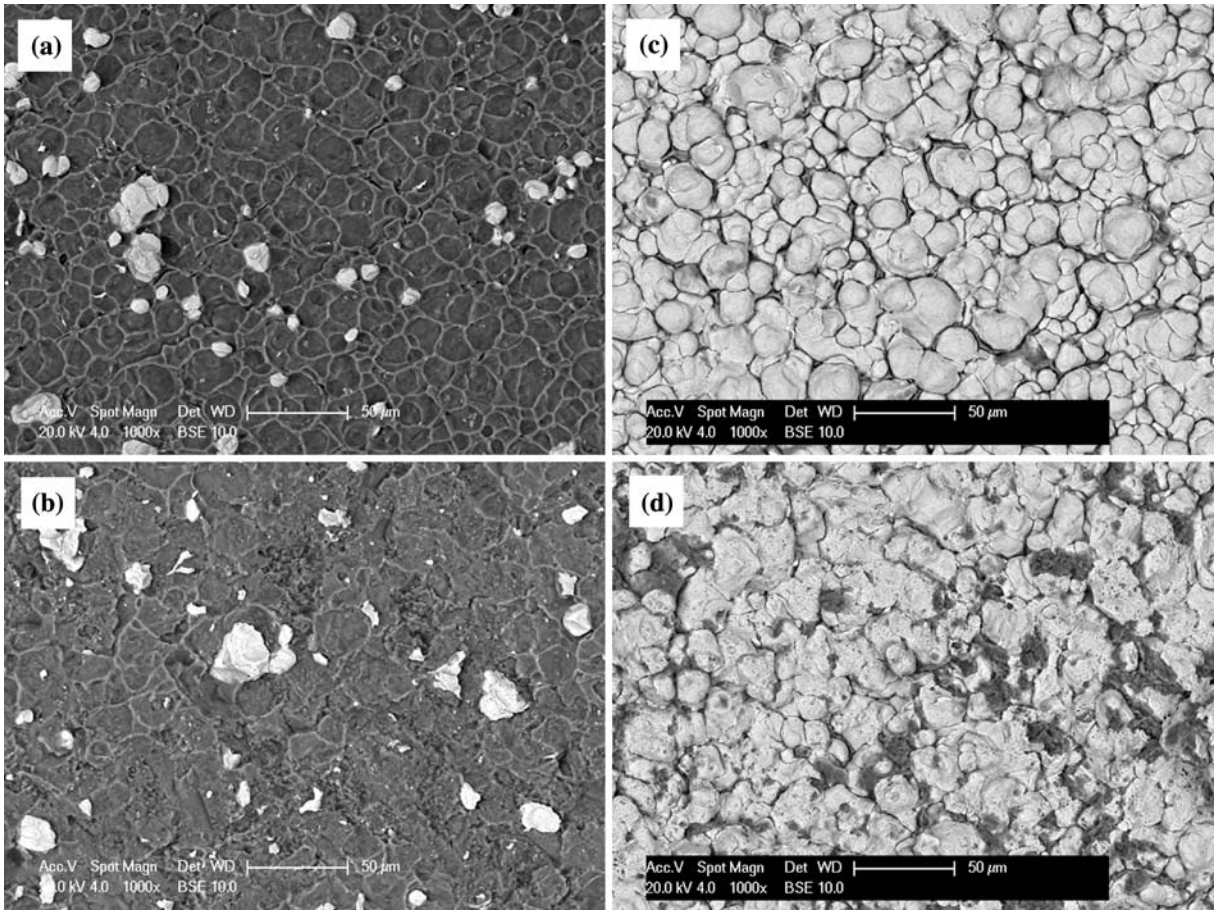

Fig. 5 Fracture surfaces, after pull-off test, of annealed Al substrate (a-b) and corresponding copper coating (c-d) with different substrate surface preparations: (a, c) ground; (b, d) grit-blasted. The bright phase is Cu and the darker one Al. The Al substrates show the presence of individual Cu particles adhered to them and the Cu coatings show Al trapped in between Cu particles

Table 3 Microscopic analysis of the material present on the substrate and on the coating after bond strength pull-off tests (all measurements were taken on BSE images with a field size of 300 × 225 µm)

Substrate surface preparation	Fraction of counter-element present			
	As-prepared substrate		Annealed substrate	
	Copper on substrate	Aluminium on coating	Copper on substrate	Aluminium on coating
Polished	0.09	0.11	N/A	N/A
Ground	0.10	0.09	0.06	0.14
Grit-blasted	0.12	0.25	0.07	0.21

The polished substrate which was annealed failed in the adhesive not at the interface

deposition), see Fig. 9. The intermetallic layer at the polished surface in the annealed sample is almost continuous (see Fig. 10a). Intermetallic coverage is lower following deposition onto the ground substrate (Fig. 10b), although here again, there is a significant increase associated with the annealing treatment following grinding. The intermetallic coverage for the grit-blasted surface is lower again, with any intermetallic being formed having a low thickness (Fig. 9c).

Table 4 presents the fraction of the interface covered with intermetallics for both as-prepared and annealed substrates for all three surface preparation methods. For the as-prepared substrates, the fraction of interface covered by intermetallics was the highest for the polished substrate. The coverage of intermetallics on the substrates which had been either ground or grit-blasted was significantly lower (and close to each other). The intermetallics formed on the grit-blasted surface showed an irregular pattern which is different from the other two surfaces.

For the substrates that were annealed after surface preparation, the fraction of interface covered with intermetallics increased significantly. Table 4 shows that the fraction of intermetallics was highest for the polished substrate, followed by the ground and then the grit-blasted surfaces. The significantly greater degree of coverage by intermetallic phases is indicative of a greater area of metal-to-metal contact (i.e., interface free from oxide) in the samples annealed following their surface preparation, as has been demonstrated previously.

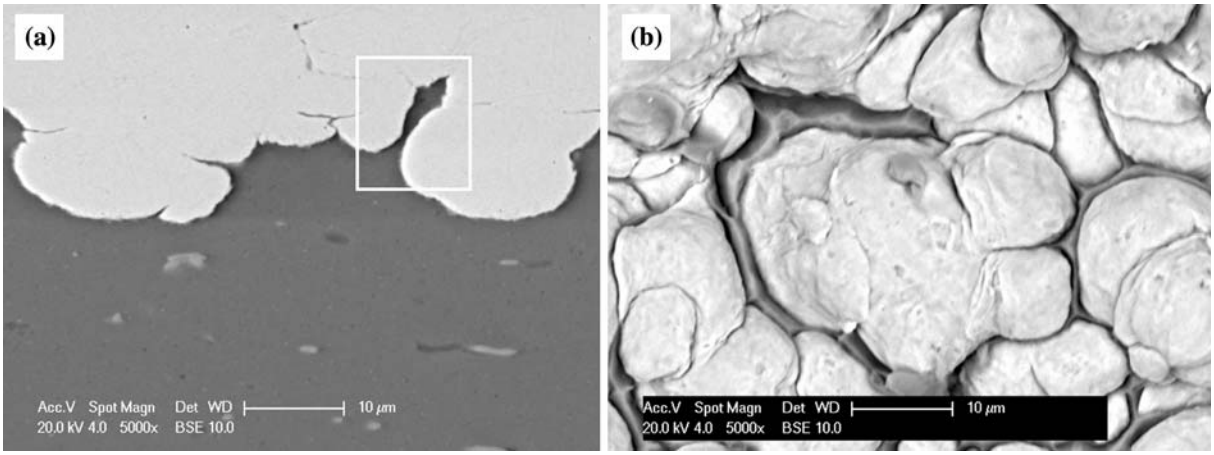

Fig. 6 (a) High magnification image of copper coating on ground and annealed aluminium substrate showing aluminium extruded in between copper particles. (b) Fracture surface (coating side) after pull-off test on the same coating-substrate combination showing rim of Al (dark) around Cu particles (bright)

4. Discussion

The discussion proceeds by treating the grit-blasted substrates separately from the other forms of preparation, since it is argued that very different phenomena are observed in the two situations.

4.1 Bond Formation: Ground Substrates and Polished Substrates

4.1.1 Experimental Observations on Bonding and Failure Mechanisms. The differences between the ground and the polished aluminium substrates are primarily in their hardness and their roughness characteristics. Table 1 shows that the near-surface hardness of the ground material is slightly less than that of the polished material (and indeed slightly less than the bulk of the sample), and that this lower hardness is retained even after annealing. However, the reasons for this reduced hardness are not clear at present. The surface roughness of the polished surface ($Ra = 0.05$ μm) is significantly less than that of the ground surface ($Ra = 0.4$ μm) (Table 1). To visualize the significance of the difference in surface profiles, line traces of both the polished and the ground surfaces (with the same magnifications in the horizontal and vertical directions) are shown in Fig. 3. In the same figure, a representation of a 15 μm copper particle on the same scale is shown. It can be seen that the polished surface may be approximated as a flat plane whereas the ground surface profile may provide some small perturbations which could affect the deformations experienced during impact.

Figures 4 and 5 show the fracture surfaces of the aluminium substrates and copper deposits (both as-prepared and annealed substrate conditions) after they had failed in the pull-off test, while Fig. 7 and 8 show cross-sections of the same deposit-substrate interfaces before testing. Deformation takes place principally in the aluminium substrate (little flattening of the copper particles is evident). Moreover, there is little evidence in these images for a significant difference between copper deposited onto a polished or a ground surface. Furthermore, ground surfaces behave in a similar manner in both as-prepared and annealed conditions despite the significant decrease in hardness brought about by annealing (106 to 35 kgf mm^{-2}). Fracture surfaces from substrates that were polished prior to application of the deposit could not be compared with and without annealing because in the former condition glue failure occurred in the pull-off test. While the small differences in surface profile compared to the particle size (as seen in Fig. 3) may explain why interface morphology is insensitive to the surface preparation method (ground vs. polished), its insensitivity to initial surface hardness is more surprising. This insensitivity to hardness (within the range examined) suggests that during the impact process, high-strain rate deformation causes significant work hardening at the interface so that the initial condition of the material before impact does not significantly affect its subsequent deformation characteristics.

The mechanism of deposit-substrate bonding in cold spraying has commonly been perceived to be primarily via the formation of metallic bonds following removal of surface oxides and creation of clean interfaces; an impacting particle causes jetting of the material which removes the surface oxide layer and a true metallurgical bond is created (Ref 4, 6-10). However, the present observations lead us to propose an additional contribution which we term ''interlocking''. It is proposed that the metal jetting due to the impact of incoming copper particles causes lips of aluminium to form which partially envelop the copper particles as shown schematically in Fig. 11. This creates mechanical interlocking of the substrate with the powder particle. Experimental evidence for this is clearly seen in the cross-sectional images of Fig. 7 and 8(a, b). Moreover, the fracture surfaces of the copper deposit following pull-off testing show regions of failed aluminium substrate outlining many of the particle

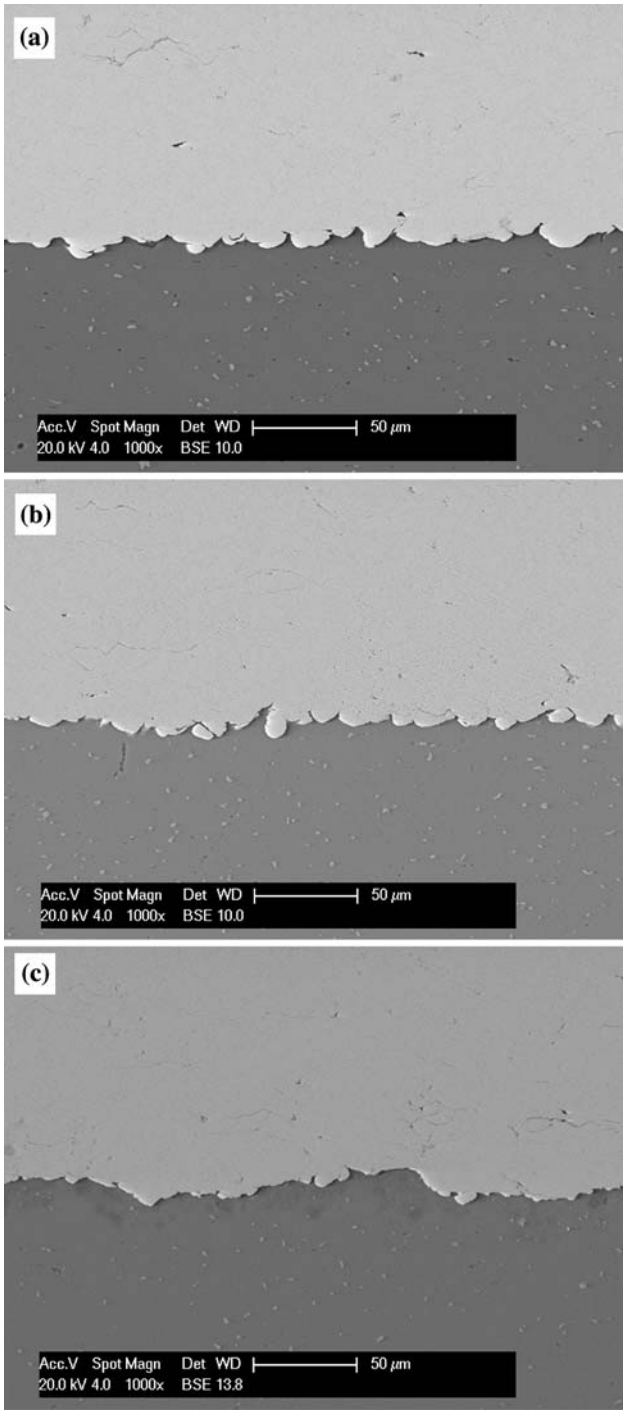

Fig. 7 BSE images of Cu (bright) on as-prepared Al substrate (dark) with (a) polished, (b) ground, (c) grit-blasted surfaces in the as-sprayed condition. Micron-sized bright particles within the Al substrate are constituent intermetallics in the 6082 alloy

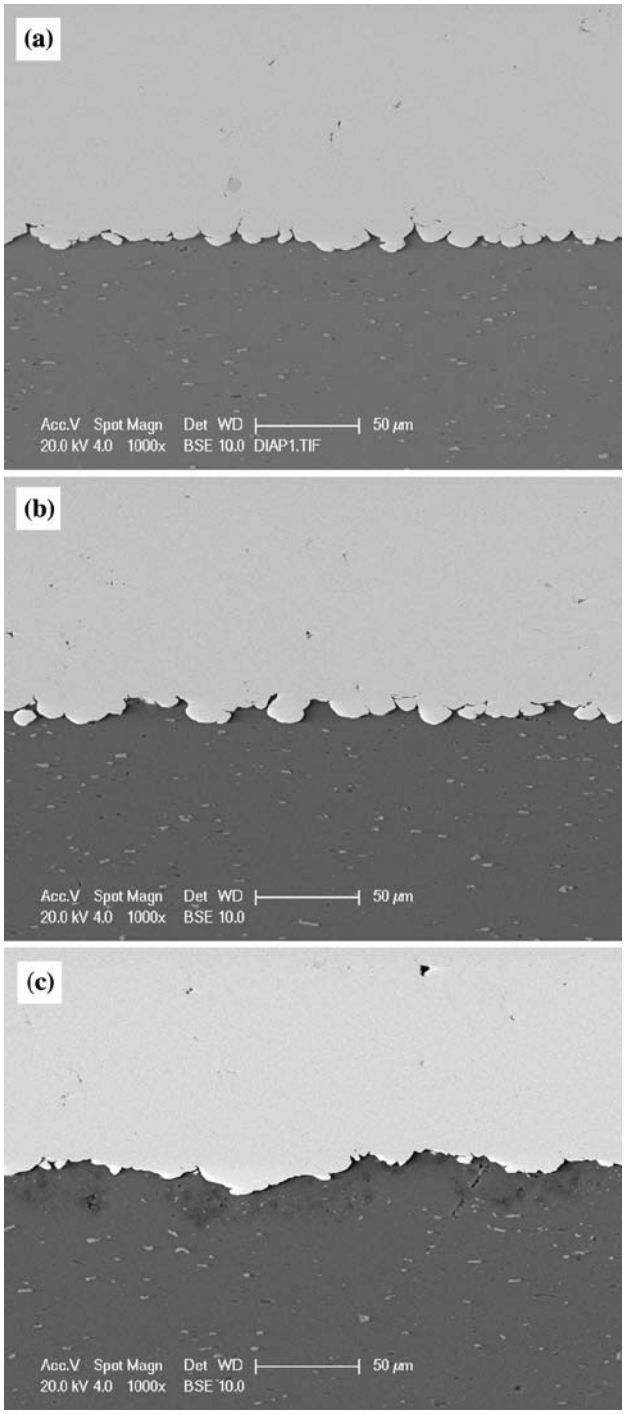

Fig. 8 BSE images of Cu (bright) on annealed Al substrate (dark) with (a) polished, (b) ground, and (c) grit-blasted surfaces in the as-sprayed condition. Micron-sized bright particles within the Al substrate are constituent intermetallics in the 6082 alloy

boundaries (Fig. 4d, e and 5c). A higher magnification image of such extruded lips of aluminium is shown in Fig. 6. It should be noted that while this mechanical interlocking of the aluminium substrate into the copper deposit is seen to be widespread, it does not exist between a significant number of the particles that can be seen on the fracture surface. Table 3 shows that when fracture surfaces are assessed the fractional area coverage of the copper coating side by these extruded lips is of the order of 0.1 and varies little with surface preparation.

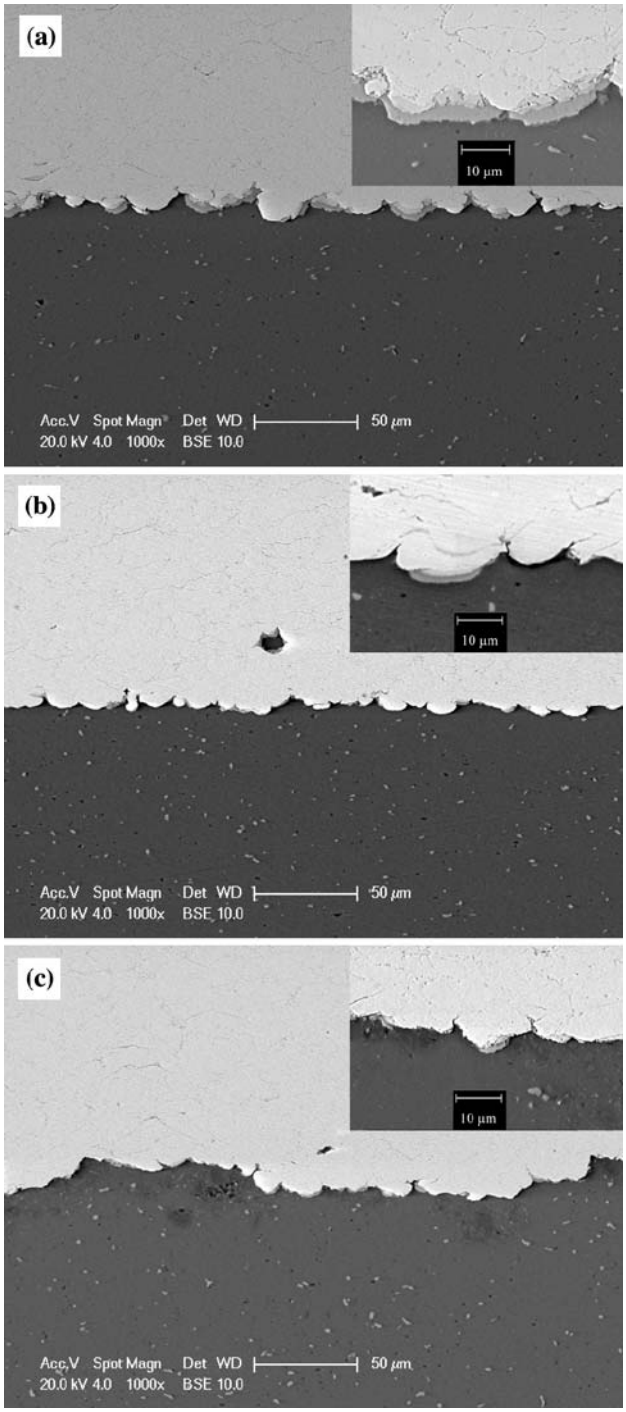

Fig. 9 BSE images of Cu (bright) on as-prepared Al substrate (dark) with (a) polished, (b) ground, and (c) grit-blasted surfaces. Samples annealed at 400 °C for 15 min following deposition. Grey contrast levels in the higher magnification insets show intermetallic that formed during annealing

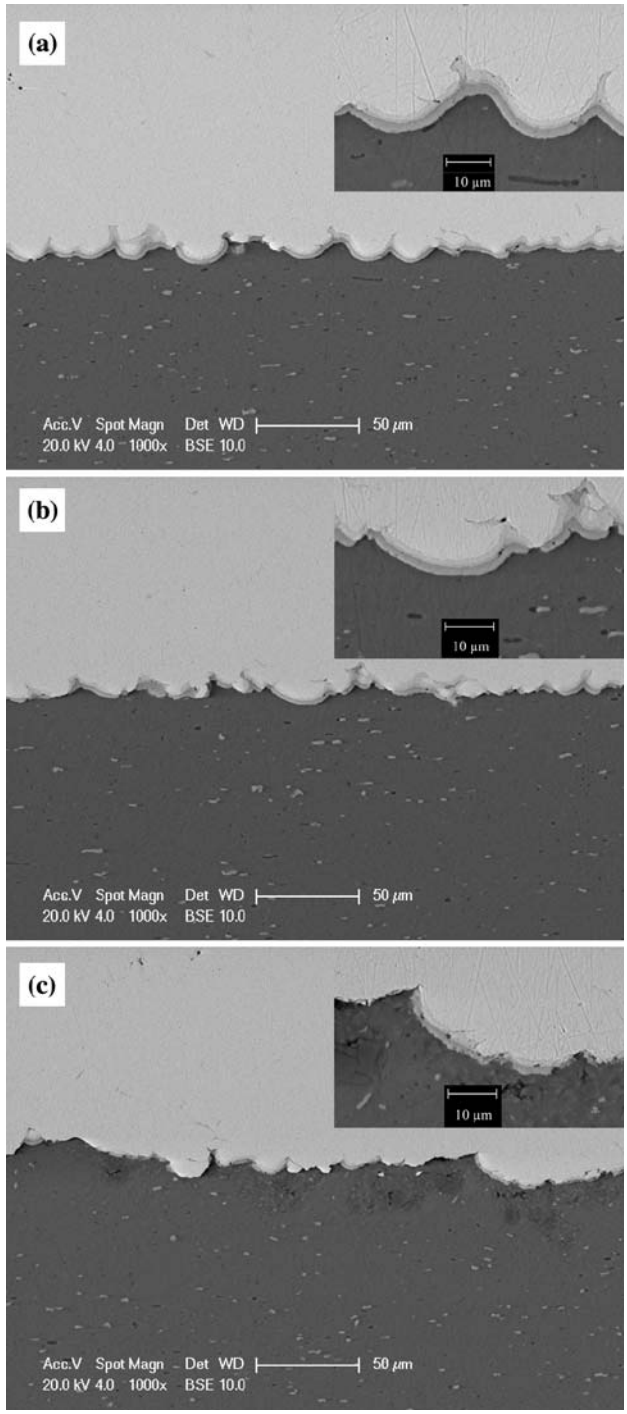

Fig. 10 BSE images of Cu (bright) on annealed Al substrate (dark) with (a) polished, (b) ground, and (c) grit-blasted surfaces. Samples annealed at 400 °C for 15 min following deposition. Grey contrast levels in the higher magnification insets show intermetallics that formed during annealing. Note the higher levels of intermetallic than in Fig. 9

In summary, it is clear that in the case of polished substrates and ground substrates there are very few morphological differences in the nature of the substrate-deposit interface as a function of whether the substrate surface is ground or polished, or whether it is hard or soft.

Turning now to a consideration of deposits that were annealed at 400 °C for 15 min, the results show some very marked differences in intermetallic formation depending

Table 4 Measurements of the fraction of the copper-aluminium interface covered with intermetallic phases after a short heat treatment of 15 min at 400 °C (all measurements taken on eight BSE images of the interface cross-section comprising approximately a 2.5 mm length of the interface)

Substrate surface preparation	Fraction of the interface covered with intermetallics	
	As-prepared substrate	Annealed substrate
Polished	0.46 ± 0.05	0.94 ± 0.01
Ground	0.27 ± 0.03	0.77 ± 0.02
Grit-blasted	0.34 ± 0.03	0.50 ± 0.05

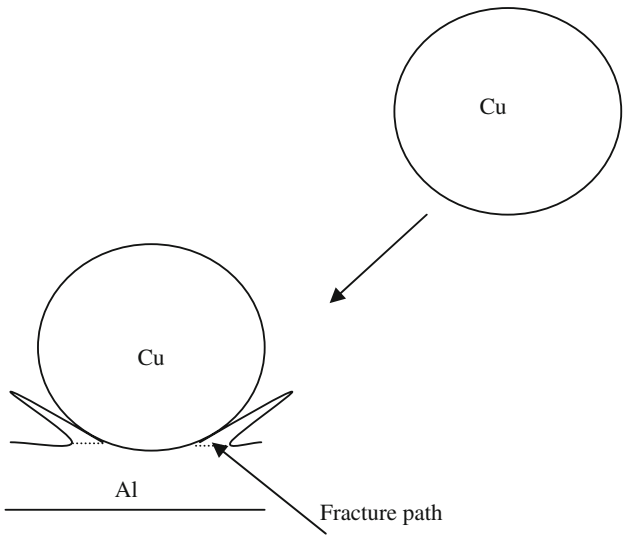

Fig. 11 Schematic illustration of jet formation on an aluminium substrate by an impinging copper particle. The jet is subsequently trapped in the copper coating by incoming copper particles. During the bond strength test fracture occurs in the aluminium jet shown by the dotted line

on substrate preparation. It is important to recollect that this annealing leads to intermetallic formation only when interdiffusion is possible, i.e., intermetallic formation acts as a marker for metallurgically clean interface regions. Figures 9 and 10 show the formation of the intermetallics, with the fractions of the interface covered with intermetallic phase presented in Table 4. On the as-prepared (polished) substrate it can be seen (Fig. 9a) that, despite significant substrate deformation (with evidence of interlocked jets of aluminium in the deposit structure), the intermetallic area fraction was only 0.46 (see Table 4). The intermetallic formation on the as-prepared ground sample (Fig. 9b) was even lower at only 0.27 (Table 4). The values for the fraction of the interface covered with intermetallics were increased to 0.94 and 0.77, respectively, for polished and ground substrates that were annealed before cold spraying.

In summary, intermetallics grow more readily on polished surfaces than on ground surfaces, and annealing of the substrate at 450 °C for 1 h prior to spraying promotes intermetallic formation in both of the surface preparation conditions. It is believed that increases in intermetallic formation must be associated with more extensive removal of oxide during the jetting process that occurs on impact. Further research is needed here but one could speculate that by annealing the substrates before cold spraying, the surface oxide is being modified; possibly being transformed from a hydrated layer to one which is corundum (α-Al_2O_3). The effect of polishing compared to grinding is less easy to rationalise at this stage.

4.1.2 Bonding Model. For the polished and ground substrates (i.e., where the adverse effects associated with the grit-blasting do not come into play), it has been demonstrated that the bonding of the coating to the substrate depends upon two primary components: (i) metallurgical bonding associated with the formation of oxide-free surfaces during jetting and (ii) mechanical interlocking of jetted material between the powder particles making up the coating structure. During bond strength testing of such coatings, decohesion of the coating from the substrate must result in failure of both the metallurgically bonded regions and the mechanically interlocked material.

To model this situation in a semi-quantitative manner, it is proposed to treat the region across the interface as a simple unidirectional composite. The composite components are the jetted material regions and the metallurgically bonded regions as shown schematically in Fig. 12.

The jetted material is regarded as an elastic solid which exhibits ductile behavior and is continuous across the interface region. The areas where the cold sprayed deposit and the substrate come into contact are treated as elastically brittle regions. The stress-strain behavior of each component is shown schematically in Fig. 13 where σ_m is the stress in the metallurgically bonded areas and σ_i the stress in the interlocked regions. σ_{mf} is the failure stress of the former and σ_i' is the stress in the interlocked regions when the metallurgical bond fails.

Using this approach, the standard theory for longitudinal tensile strength of a long fibre reinforced composite can be applied.

The stress in the composite, σ_c, is given by

$$\sigma_c = \sigma_m f_m + \sigma_i f_i \quad \text{(Eq 1)}$$

where f_m and f_i are the area fraction of the interface corresponding to metallurgical bond and interlocked material, respectively.

If we assume that the interlocked material is ductile but the metallurgical bond fails in a brittle manner at a critical stress σ_{mf} (see Fig. 13), then the stress in the composite, σ_c', when this failure occurs is given by

$$\sigma_c' = \sigma_{mf} f_m + \sigma_i' f_i \quad \text{(Eq 2)}$$

Assuming that $f_m + f_i = 1$, then

$$\sigma_c' = (\sigma_{mf} - \sigma_i')\, f_m + \sigma_i' \quad \text{(Eq 3)}$$

When the metallurgically bonded region fails, all the load is transferred to the interlocked material. The maximum

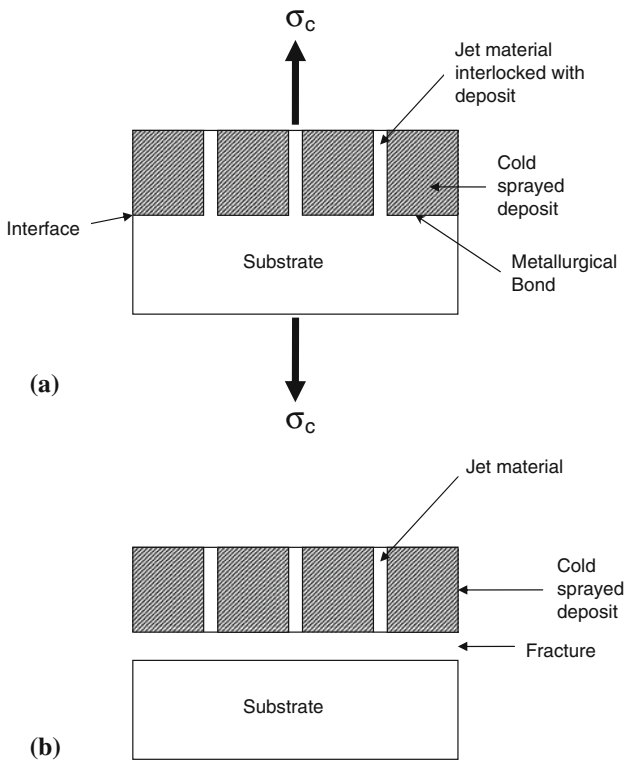

Fig. 12 Schematic diagram of deposit-substrate debonding at the interface, indicating failure of both the interlocked substrate and the regions of deposit-substrate metallurgical bonding; (a) prior to failure and (b) post failure

composite stress that can be transferred to interlocked material is given by

$$\sigma_c' = \sigma_{ui} f_i = \sigma_{ui}(1 - f_m) \quad \text{(Eq 4)}$$

where σ_{ui} is the tensile strength of the interlocked material (Fig. 13).

Classically, Eq 3 and 4 are represented by plotting stress as a function of f_m as shown by the schematic diagram in Fig. 14.

However, in the present situation, the equations need to be modified to take account of the fact that the true metallurgically bonded area fraction, f_m^T, differs from the apparent contact area fraction, f_m.

We define f_m as the apparent metallurgically bonded area such that $f_m + f_i = 1$ and take the true metallurgically bonded area to be given by

$$f_m^T = f_m \times f_{int} \quad \text{(Eq 5)}$$

where f_{int} is the measured area fraction of intermetallic coverage as presented in Table 4.

So for metallurgical bond failure Eq 2 is modified to become

$$\sigma_c' = \sigma_{mf} f_m f_{int} + \sigma_i'(1 - f_m) = (\sigma_{mf} f_{int} - \sigma_i') f_m + \sigma_i' \quad \text{(Eq 6)}$$

Clearly for a given value of f_m, changes in f_{int} will affect the position of the composite failure strength line in relation to the line for composite strength that can be supported by interlocked material (Eq 4). The behaviors of Eq 3, 4 and 6 are illustrated schematically in Fig. 14. It is evident that for a chosen value of f_m (shown as f_m' in Fig. 14) there are two possible types of behavior.

Case 1 Below a critical value for f_{int}, the composite failure strength will be controlled by failure of the interlocked material and will be constant at the value σ_c^* shown in Fig. 14.

Case 2 Above a critical value for f_{int}, the composite failure strength will be governed by Eq 6.

It is now possible to apply this model to the experimental data reported in Table 2-4. The bond strength is almost constant for as-prepared polished, as-prepared ground, and annealed ground substrates (Table 2). For these conditions the fraction of interlocked material, f_i, also remains constant at about 0.12 (this is the fraction of aluminium on the copper coating). For these three conditions, the f_{int} value varies from 0.27 to 0.77 but with no apparent effect on the bond strength. Therefore we can explain this on the basis that these values of f_{int} are such that failure strength is controlled as in case 1 above. Taking the fraction of interlocked material, f_i, to be 0.11 and estimating the value of σ_{ui} to be 432 MPa (1/3 of the hardness of the 6082 alloy cold rolled to a strain of 360%), we find that σ_c' is of the order of 48 MPa from Eq 4. This is in good agreement with the observed values, given the approximate nature of the analysis.

In the case of the polished sample which was annealed before deposition of copper, it is argued that f_{int} had increased to such an extent that failure occurred according to the behavior ascribed to case 2 above. The bond strength could not be measured since the fracture occurred in the adhesive at an applied stress of 69 MPa. We need to know the Young's moduli of both the interlocked and metallurgically bonded regions in order to determine how the stress is distributed between the two components of the composite. If they are taken to be equal, and if f_{int} is taken to be 1, then a lower bound value for σ_{mf} is 69 MPa. In practice, f_{int} is less than 1 and the metallurgically bonded regions are likely to be of higher stiffness (being composed of aluminium and copper) than the interlocked regions (which are composed of aluminium), and so the actual value for σ_{mf} will probably be in excess of this value.

4.2 Bond Formation: Grit-Blasted Substrates

In considering the behavior of grit-blasted surfaces, the morphology of fracture surfaces following the pull-off test will be examined first of all and this will be followed by a consideration of how this might modify bonding during cold spraying.

4.2.1 Morphological Features Arising from Impact. The principal features due to impact on a grit-blasted surface seen in Fig. 4(c) and 7(c) appear very similar to those observed following impact on the grit-blasted and

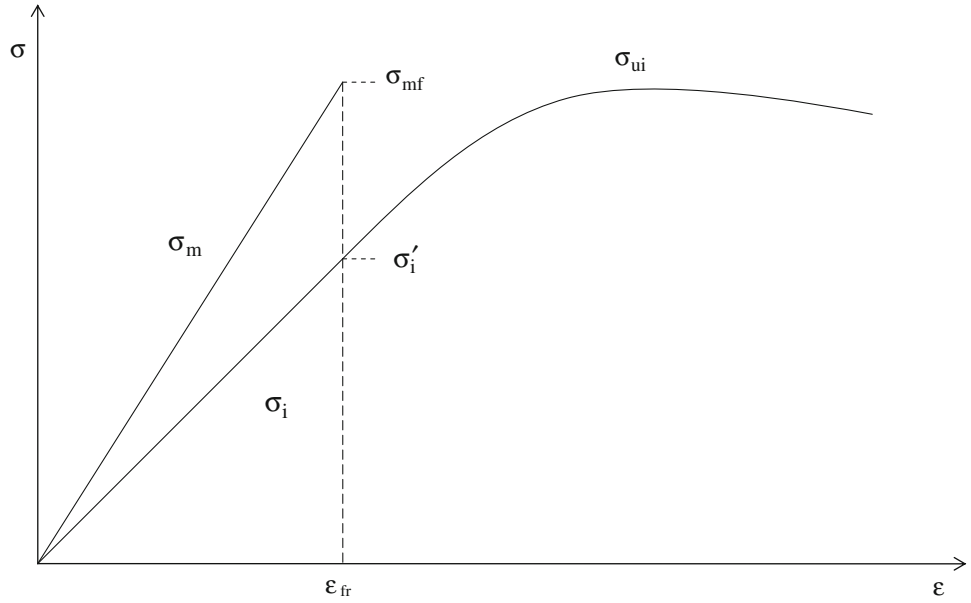

Fig. 13 Stress-strain behavior of metallurgically bonded area and mechanically interlocked area assuming that the metallurgically bonded area exhibits brittle behavior and that the mechanically interlocked area exhibits ductile behavior

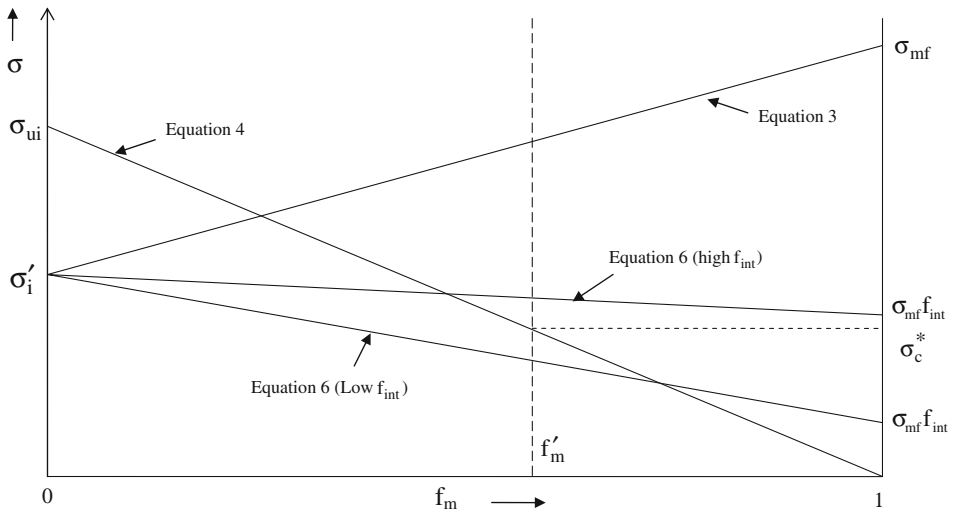

Fig. 14 Failure stresses associated with the different failure modes as indicated in Eq 3, 4 and 6 as a function of the fraction of the metallurgically bonded material. The lines for Eq 6 are shown for two different values of f_{int}

annealed surface (Fig. 5b and 8c), despite the fact that the annealed surface is significantly less hard, namely 50 kgf mm^{-2}, compared with 180 kgf mm^{-2}. It is evident that a very large proportion of the copper particles that impacted on the grit-blasted surfaces developed a rough and pitted appearance which is mirrored by the appearance of the substrate (i.e., the aluminium side of the fracture surfaces). These features are clearly attributable to the use of the Al_2O_3 grit in the preparation stage and it would appear that under the conditions used to prepare these substrates, the brittle Al_2O_3 fragmented and some of these fine fragments became embedded in the soft aluminium substrate. In the cross-sectional BSE images of deposits on grit-blasted substrates (Fig. 7c, 8c, 9c, and 10c), evidence of a slightly lower contrast material just below the substrate surface can be seen, along with some porosity in that zone. This material is believed to be embedded Al_2O_3 fines, a hypothesis which is consistent with EDX measurements which indicated no other elements than aluminium and oxygen in this region. The porosity observed was typically less than 5 μm in size, which is much less than the size of the original blast-media particle size, but similar to that of the embedded fines.

The similar behavior of as-prepared and annealed substrates in terms of deformation characteristics confirms the previous observation on ground/polished surfaces that very low strain rate hardness measurements cannot adequately predict the behavior of surfaces under the high rates of strain associated with impact. The hardness reduction that does take place is probably due to the high-temperature annealing treatment allowing classical recovery or recrystallization processes to occur in the aluminium alloy. The Al_2O_3 fines contribute to the near-surface hardness of the aluminium since they act as a dispersion strengthening phase. This contribution is of course not affected by annealing and is presumably responsible for the higher near-surface hardness (Table 1) of the annealed, grit-blasted substrate compared to other surface preparations.

4.2.2 Influence of Grit-Blasting on Jetting and Bond Strength Measurements. A key question for bond formation during cold spraying is how the surface morphology, near-surface hardness and microstructure will affect jetting phenomena during impact. The grit-blasting changes the profile of the substrate surface with a significant increase in Ra compared to the other two preparation processes (Table 1). Figure 2 shows the surface profile with Fig. 3 showing the profile with the same magnifications in horizontal and vertical directions, along with a typical powder particle size. In this latter image, it can be seen therefore that the local conditions during impact of powder particles onto a grit-blasted substrate will be very variable. The flattening of the copper particles seen in Fig. 7 and 8 indicates that the surface material in the grit-blasted substrate is more resistant to deformation under impact conditions, and that jetting during impact will be restricted. There is significantly less evidence of jetted substrate material forming a mechanical interlock with the deposit for the grit-blasted substrate than for the other two surface preparation methods. This limitation of jetting during impact also affects the efficacy of removal of surface oxide layers during impact (and thus the efficacy of any metallurgical bonding between the copper and aluminium). Figures 9(c) and 10(c) show the interfaces between the aluminium and copper following intermetallic growth. It can be seen that the intermetallic growth is limited in both cases. In the non-annealed samples (Fig. 9), the intermetallic growth is similar to that observed on the ground sample and slightly lower than that on the polished sample (see Table 4). However, while the coverage of intermetallic increased for the grit-blasted samples with annealing (from approximately 34 to 50%), this was much less significant than the effect that the annealing had on the other two sample preparation types (see Table 4).

The bond strength in pull-off testing of the samples with as-prepared grit-blasted substrates was significantly lower than those observed with the other two preparation types (around 35 MPa as compared to around 56 MPa). Figure 4(f) shows that, unlike the deposit surfaces from the other two types (Fig. 4d, e), significant regions of the aluminium substrate were retained on the surface. This indicates that fracture is occurring in the aluminium substrate, and it is proposed that fracture is being promoted in the zone which contains the embedded grit-blasting fines, it being weakened by the presence of these fines. The same effect is observed following fracture of the deposit from the grit-blasted surface that had been annealed before spraying (Fig. 5d), but to a lesser degree. However, it is observed that the bond strength for the grit-blasted samples was significantly increased from around 35 MPa to around 57 MPa by the annealing process (see Table 2). The fraction of intermetallics has also increased significantly with annealing of the substrate, from 34 to 50% (see Table 4). Thus, although the substrate surface is roughened by the blasting process, the embedment of grit fines in the surface results in a surface which is much more resistant to high strain rate deformation (even if the effects of work hardening are eliminated). This results in less jetting of the aluminium during impact and thus to a restriction in the formation of metallurgical bonds between the deposit and substrate. The embedded grit results in fracture actually within the substrate following pull-off testing.

In summary, grit-blasting has been seen to be detrimental to the bonding process in the system comprising copper particles and an aluminium substrate examined in the present study. It must be recognized, however, that due to the low hardness of the substrate, the tendency for grit fines to embed during blasting will be relatively high compared to materials such as steel or titanium alloys. Grit-blasting of other, harder substrates may not result in such significant embedment of fines, and thus the adverse effects of the blasting process observed in this work may not be universal.

5. Conclusion

The bonding mechanisms operating in cold spraying of copper onto an aluminium alloy substrate have been investigated experimentally as a function of the different surface preparation procedures for the substrate, namely polished, ground and grit-blasted substrate surfaces. In addition, some substrates were annealed following surface preparation to allow a separation of the effects of work hardening during preparation from those of changes in surface morphology. A bonding mechanism has been proposed to explain the observations which utilizes two mechanisms of bonding, namely that of metallurgical bonding between the substrate and the coating and that of material extruded from the substrate during impact of the particles which is then interlocked within the coating structure (termed interlocked material). The contributions of these two mechanisms to the observed bond strength are rationalized in terms of a modified composite theory.

The efficiency of metallurgical bonding was assessed via a relatively new intermetallic growth method. When the efficiency of metallurgical bonding was low, the coating-substrate adhesive strength was controlled by the strength of the interlocked material. Simple calculations based upon the area fraction of interlocked material at the

interface along with the strength of that material show a good correlation with the observed bond strengths in these cases. However, when the efficiency of the metallurgical bonding was increased (when spraying aluminium onto a polished and annealed aluminium alloy substrate), the strength was then dictated by the metallurgically bonded material.

Coating-substrate adhesion following spraying onto a grit-blasted surface (whether or not the effects of work hardening had been removed by annealing) was significantly reduced by grit embedment into the aluminium surface during blasting. It is postulated that the grit-blasted surface also restricted the jet formation upon impact of the copper particles which resulted in less successful removal of oxide from the interface and hence a weaker metallurgical bond. Also, the increased strength of the particulate strengthened substrate material resisted formation of interlocked material between the coating and substrate, and thus again resulted in a reduction in observed bond strength.

Acknowledgments

T. Hussain acknowledges financial support from the University of Nottingham as Overseas Research Studentship (ORS) and an industrial CASE studentship from TWI Ltd., UK.

References

1. R.C. Dykhuizen and M.F. Smith, Gas Dynamic Principles of Cold Spray, *J. Therm. Spray Technol.*, 1998, **7**(2), p 205-212
2. H. Assadi, F. Gartner, T. Stoltenhoff, and H. Kreye, Bonding Mechanism in Cold Gas Spraying, *Acta Mater.*, 2003, **51**(15), p 4379-4394
3. T. Schmidt, F. Gartner, H. Assadi, and H. Kreye, Development of a Generalized Parameter Window for Cold Spray Deposition, *Acta Mater.*, 2006, **54**(3), p 729-742
4. M. Grujicic, J.R. Saylor, D.E. Beasley, W.S. DeRosset, and D. Helfritch, Computational Analysis of the Interfacial Bonding Between Feed-Powder Particles and the Substrate in the Cold-Gas Dynamic-Spray Process, *Appl. Surf. Sci.*, 2003, **219**(3-4), p 211-227
5. T. Stoltenhoff, H. Kreye, and H.J. Richter, An Analysis of the Cold Spray Process and Its Coatings, *J. Therm. Spray Technol.*, 2002, **11**(4), p 542-550
6. A.O. Tokarev, Structure of Aluminum Powder Coatings Prepared by Cold Gasdynamic Spraying, *Met. Sci. Heat Treat.*, 1996, **38**(3-4), p 136-139
7. T.H. Van Steenkiste, J.R. Smith, and R.E. Teets, Aluminum Coatings via Kinetic Spray with Relatively Large Powder Particles, *Surf. Coat. Technol.*, 2002, **154**(2-3), p 237-252
8. M. Grujicic, C.L. Zhao, W.S. DeRosset, and D. Helfritch, Adiabatic Shear Instability Based Mechanism for Particles/Substrate Bonding in the Cold-Gas Dynamic-Spray Process, *Mater. Design*, 2004, **25**(8), p 681-688
9. W.Y. Li, H.L. Liao, C.J. Li, H.S. Bang, and C. Coddet, Numerical Simulation of Deformation Behavior of Al Particles Impacting on Al Substrate and Effect of Surface Oxide Films on Interfacial Bonding in Cold Spraying, *Appl. Surf. Sci.*, 2007, **253**(11), p 5084-5091
10. R.C. Dykhuizen, M.F. Smith, D.L. Gilmore, R.A. Neiser, X. Jiang, and S. Sampath, Impact of High Velocity Cold Spray Particles, *J. Therm. Spray Technol.*, 1999, **8**(4), p 559-564
11. T.S. Price, P.H. Shipway, D.G. McCartney, E. Calla, and D. Zhang, A Method for Characterizing the Degree of Inter-Particle Bond Formation in Cold Sprayed Coatings, *J. Therm. Spray Technol.*, 2007, **16**(4), p 566-570
12. V.K. Champagne, D. Helfritch, P. Leyman, S.G. Ahl, and B. Klotz, Interface Material Mixing Formed by the Deposition of Copper on Aluminum by means of the Cold Spray Process, *J. Therm. Spray Technol.*, 2005, **14**(3), p 330-334
13. K. Balani, A. Agarwal, S. Seal, and J. Karthikeyan, Transmission Electron Microscopy of Cold Sprayed 1100 Aluminum Coating, *Scr. Mater.*, 2005, **53**(7), p 845-850
14. C. Borchers, F. Gartner, T. Stoltenhoff, and H. Kreye, Microstructural Bonding Features of Cold Sprayed Face Centered Cubic Metals, *J. Appl. Phys.*, 2004, **96**(8), p 4288-4292
15. R.C. McCune, W.T. Donlon, O.O. Popoola, and E.L. Cartwright, Characterization of Copper Layers Produced by Cold Gas-Dynamic Spraying, *J. Therm. Spray Technol.*, 2000, **9**(1), p 73-82
16. T. Marrocco, D.G. McCartney, P.H. Shipway, and A.J. Sturgeon, Production of Titanium Deposits by Cold-Gas Dynamic Spray: Numerical Modeling and Experimental Characterization, *J. Therm. Spray Technol.*, 2006, **15**(2), p 263-272
17. J.W. Wu, J.G. Yang, H.Y. Fang, S. Yoon, and C. Lee, The Bond Strength of Al-Si Coating on Mild Steel by Kinetic Spraying Deposition, *Appl. Surf. Sci.*, 2006, **252**(22), p 7809-7814
18. H. Mäkinen, J. Lagerbom, and P. Vuoristo, Adhesion of Cold Sprayed Coatings: Effect of Powder, Substrate, and Heat Treatment, *Thermal Spray: Global Coating Solutions*, B.R. Marple, M.M. Hyland, Y. Lau, C. Li, R.S. Lima, and G. Montavon, Eds., May 14-16, 2007 (Beijing, People's Republic of China), ASM International, 2007, p 31-36
19. K. Sakaki, T. Tajima, H. Li, S. Shinkai, and Y. Shimizu, Influence of Substrate Conditions and Traverse Speed on Cold Sprayed Coatings, *Thermal Spray: Advances in Technology and Application*, May 10-12, 2004 (Osaka, Japan), ASM International, 2004, p 358-362
20. P. Richer, B. Jodoin, K. Taylor, E. Sansoucy, M. Johnson, and L. Ajdelsztajn, Effect of Particle Geometry and Substrate Preparation in Cold Spray, *Thermal Spray: Exploring Its Surfacing Potential*, E. Lugscheider, Ed., May 2-4, 2005 (Basel, Switzerland), ASM International, 2005
21. T. Stoltenhoff, C. Borchers, F. Gartner, and H. Kreye, Microstructures and Key Properties of Cold-Sprayed and Thermally Sprayed Copper Coatings, *Surf. Coat. Technol.*, 2006, **200**(16-17), p 4947-4960
22. F.A. Calvo, A. Urena, J.M.G. Desalazar, and F. Molleda, Special Features of the Formation of the Diffusion Bonded Joints Between Copper and Aluminum, *J. Mater. Sci.*, 1988, **23**(6), p 2273-2280
23. I. Manna and J.D. Majumdar, Enhanced Kinetics of Diffusion Coating of Aluminum on Copper by Boundary Diffusion, *J. Mater. Sci. Lett.*, 1993, **12**(12), p 920-922
24. Y. Funamizu and K. Watanabe, Interdiffusion in Al-Cu System, *Trans. Jpn. Inst. Met.*, 1971, **12**(3), p 147-152
25. D. Zhang, P.H. Shipway, and D.G. McCartney, Cold Gas Dynamic Spraying of Aluminum: The Role of Substrate Characteristics in Deposit Formation, *J. Therm. Spray Technol.*, 2005, **14**(1), p 109-116
26. E. Calla, ''Cold Gas Spraying of Copper and Tin onto Metallic and Non Metallic Substrates,'' Ph.D. Thesis, University of Nottingham, 2005
27. R.C. Dykhuizen and R.A. Neiser, Optimizing the Cold Spray Process, *Thermal Spray: Advancing the Science and Applying the Technology*, B.R. Marple and C. Moreau, Eds., May 5-8, 2003 (Orlando, FL), ASM International, 2003, p 19-26
28. C. Borchers, F. Gartner, T. Stoltenhoff, H. Assadi, and H. Kreye, Microstructural and Macroscopic Properties of Cold Sprayed Copper Coatings, *J. Appl. Phys.*, 2003, **93**(12), p 10064-10070